Electron traps related to oxygen vacancies in $PbWO_4$

V. V. Laguta,[1] M. Martini,[2] A. Vedda,[2] E. Rosetta,[2] M. Nikl,[3] E. Mihóková,[3] J. Rosa,[3] and Y. Usuki[4]
[1]*Institute for Problems of Material Science, Ukrainian Academy of Sciences, Krjijanovskogo 3, 03142 Kiev, Ukraine*
[2]*INFM and Dept. of Materials Science, University of Milano-Bicocca, Via Cozzi 53, 20125 Milan, Italy*
[3]*Institute of Physics AS CR, Cukrovarnicka 10, 162 53 Prague, Czech Republic*
[4]*Furukawa LtD.,20 Kodate Kamiyoshima,970-1153 Iwaki, Japan*
(Received 26 November 2002; revised manuscript received 11 March 2003; published 15 May 2003)

Four types of electron traps in $PbWO_4$, based on regular W sites perturbed by oxygen vacancies, are identified by electron spin resonance (ESR). The analysis of the ESR spectra parameters (g-factor values and principal-axes orientations) shows that the revealed centers are $(WO_3)^-$ vacancy-containing complex anions associated with a defect in the Pb sublattice: $(WO_3)^-$-A_{Pb} complexes. Two of the centers (W_1 and W_2) are thermally stable up to 350–370 K, while the other two (W_3 and W_4) are stable only up to 270–290 K. Above these temperatures the trapped electrons become free and recombine with localized holes, giving rise to a composite TSL glow peak at $T \approx 323$ K (characterized by a trap depth of 0.9 eV evaluated by the initial rise method) and to a weaker TSL structure at $T \approx 365$ K. The correspondence between $(WO_3)^-$-A_{Pb} centers and TSL peaks is supported by their similar room temperature time decays, and by the similar dependences of ESR and TSL signals upon annealing treatments. A scheme of local electronic levels in the band gap of $PbWO_4$ is proposed.

DOI: 10.1103/PhysRevB.67.205102 PACS number(s): 61.72.Ji, 61.82.Ms, 76.30.Mi, 78.60.Kn

I. INTRODUCTION

Lead tungstate [$PbWO_4$ (PWO)] became a subject of intense studies in the 1990s, when it was selected as a scintillator for coming applications in electromagnetic calorimeter detectors for high-energy-physics experiments.[1] Apart from detailed reports on luminescence and scintillation characteristics, the nature and role of various defect states in the processes of energy transfer and storage remained a subject of debate (for a review, see Ref. 2). Trying to provide a microscopic interpretation of the radiation induced optical absorption, several mechanisms were suggested and various point-defect configurations were considered for the free-charge-carrier capture and color-center creation. For instance, simple hole centers (Pb^{3+} and O^-) as well as electron centers (F and F^+) were assumed to explain radiation-induced-absorption spectra at room temperature.[3] Oxygen vacancies were considered as parent sites for electron traps in the radiation-damage mechanism at room temperature.[4] Other authors considered oxygen bivacancies[5] as electron traps and bi-(O^-) hole centers coupled to lead vacancies.[5,6] Finally, the cluster of two lead ion vacancies and one oxygen vacancy was suggested as a parent site for the capture of two holes at neighboring oxygen anions, and such a color center was ascribed to the radiation induced absorption band peaking at 350 nm.[7] Such a triple-vacancy center was found to be stable in theoretical calculations.[8] The electronic structure, the energy position within the band gap, and the configuration of oxygen vacancy-based defects were also treated theoretically.[9,10] It was concluded that the d states of tungsten, due to the missing oxygen in the WO_4 tetrahedron, are lowered and fall into the forbidden gap. However, hypotheses dealing with the nature and configuration of color centers should be experimentally verified by means of a method, like electron spin resonance (ESR), sensitive to monitor unpaired spins of electron/holes captured at such color centers.

A systematic study of the processes of charge carrier localization in PWO was recently initiated by some of us. It was found that electron autolocalisation in the PWO lattice [polaronic $(WO_4)^{3-}$ center] occurs after ultraviolet light irradiation below 40 K (see Refs. 11 and 12). Electrons thermally freed at about 50 K from the $(WO_4)^{3-}$ center radiatively recombine with holes localized nearby giving the excitonlike emission in the blue spectral region.[13] They can also be retrapped by a deeper lattice defect, namely, by a Pb^{2+} cation perturbed by an oxygen vacancy (V_O).[14,15] Above $T \approx 180$ K, such Pb^+-(V_O) centers are thermally ionized, giving rise to a thermally stimulated luminescence (TSL) glow peak.[15] Trivalent ion (La^{3+}) doping of PWO results in the stabilization of the autolocalized electron in La^{3+}-$(WO_4)^{3-}$ center up to 100 K and its thermal disintegration is again accompanied by a TSL peak around this temperature.[16]

In this work we present a further complementary ESR and TSL study on high-purity PWO single crystals. In particular, we focus on the photoinduced defects that are thermally stable at $T > 260$ K and therefore can be directly involved in radiation-damage processes of PWO at room temperature. Some of the preliminary results related to the defects studied here have been briefly published previously.[17,18]

II. SAMPLES AND EXPERIMENTAL DETAILS

$PbWO_4$ single crystals were grown by the Czochralski method in air using the third crystallization method.[19] Such a method consists of twice regrowing the crystal, when previously grown crystal(s) is (are) used to obtain the melt. The crystals were slightly doped with Rb (0.5 ppm in the sample) and also contained Cu ($\sim 1-2$ ppm). Samples for ESR measurements, $2.4 \times 2.6 \times 8$ mm^3, were cut in the (001) and (100) planes, while for TSL measurements, polished samples 1 mm thick and approximately 1 cm^2 in area were used.

High-temperature-annealing treatments were performed in inert-gas (Ar) or oxygen atmospheres. The samples were heated at a rate of 10–12 °C/min up to 950 °C, held at that temperature for 4 h, and cooled to room temperature at a rate of approximately 12 °C/min. The ESR measurements were performed at 9.21 GHz and at temperatures from 4 to 100 K. A mercury high pressure arc lamp and a halogen tungsten lamp were used for an optical irradiation of the samples. TSL measurements were performed following x-ray irradiation (Machlett OEG50 x-ray tube operated at 30 kV) at 293 K. The TSL signal was detected by an EMI 9635QB photomultiplier tube. Wavelength-resolved measurements were also performed by a home made TSL apparatus allowing measurement of the TSL intensity both as a function of temperature and wavelength. The detector was a double stage microchannel plate followed by a diode array; the dispersive element was a 140 lines/mm holographic grating, the detection range being 200–800 nm. In both cases, a heating rate of 1 K/s was adopted.

III. EXPERIMENTAL RESULTS AND THEIR INTERPRETATION

A. ESR spectra

Before illumination, the samples manifest only weak spectra of Ce^{3+} and Nd^{3+} in agreement with results of Rosa *et al.*[20] After illumination by UV light ($\lambda \simeq 260$–330 nm) at $T \simeq 290$ K (room temperature) (RT) new ESR spectra appear [Fig. 1(a)]. Alternatively, these new spectra can be produced by ultraviolet irradiation at low temperatures and subsequent heating to $T \simeq 260$–300 K (Fig. 2). The same effect can be obtained under x-ray irradiation. The ESR signal reaches its maximum at $T = 12$–16 K. As temperature increases, the intensity rapidly decreases due to temperature dependence of the spin-lattice relaxation, and the ESR spectra completely vanish at $T > 45$ K. It will be shown below that these new ESR spectra belong to W^{5+} lattice ions with different surroundings.

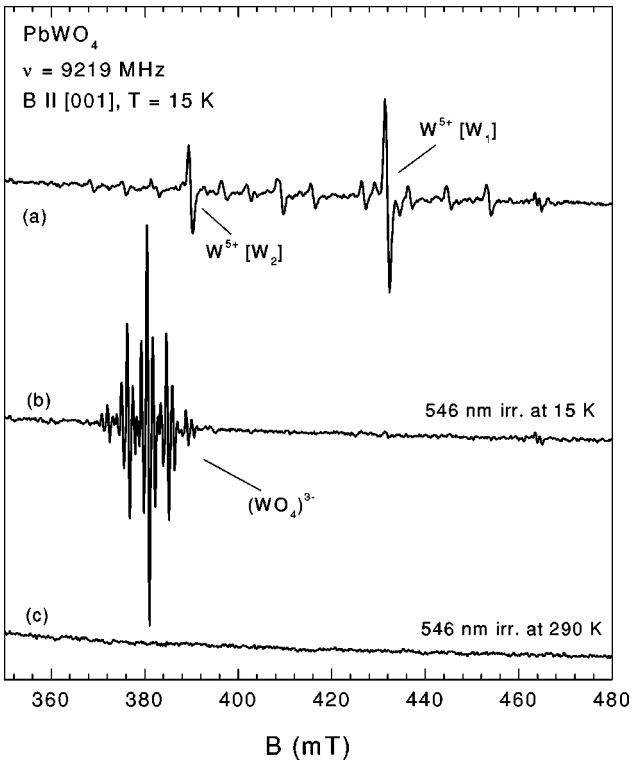

FIG. 1. ESR spectra at 15 K in $PbWO_4$ after ultraviolet (UV) irradiation at 290 K, curve (a). Influence of subsequent irradiation by the 546-nm line of an Hg-arc lamp selected by an interference narrow band-pass (10-nm) filter at 15 K [curve (b)] and at 290 K [curve (c)].

The W^{5+} spectra can be completely erased by either green light illumination [Figs. 1(b) and 1(c)] or temperature increase (Fig. 2). Note that the effect of green light illumination is different at low ($T \lesssim 40$ K) temperatures and at RT: while irradiation at 15 K converts the W^{5+} centers into polaronic $(WO_4)^{3-}$ centers, irradiation at RT leads to recombination of freed electrons with localized holes and electron traps are completely erased.

Under gradual heating from 260 to 300 K at least four types of W^{5+} centers with different temperature stability and spectral parameters can be distinguished (Fig. 2). We denote them W_1, W_2, W_3, and W_4. The concentrations of W^{5+} centers vary in different samples and are estimated around only several atomic ppm. The detailed analysis of the W^{5+} ESR spectra evidences the superhyperfine (shf) structure

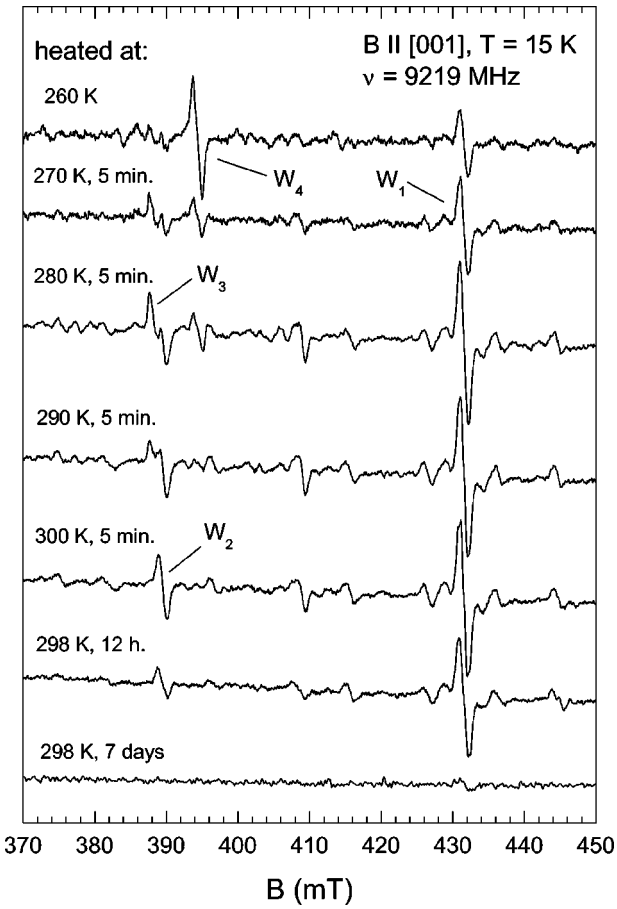

FIG. 2. Influence of temperature increase on the UV light induced paramagnetic centers in $PbWO_4$.

originating from ^{207}Pb nuclei. The ^{207}Pb isotope, whose natural abundance is 22%, possesses a nuclear spin $I=1/2$, resulting in the observation of shf doublets and small-intensity triplets (when an electron simultaneously interacts with two isotopes), as indicated in Fig. 3 for two (W_1 and W_2) centers. The spectra of other two centers, non shown here, have approximately the same shf structure and, again, all visible shf lines are related to ^{207}Pb nuclei. In contrast to the unperturbed $(WO_4)^{3-}$ polaronic center, where the shf pattern arises from the interaction of a paramagnetic ion with two sets (4 + 4) of equivalent Pb nuclei [see Fig. 1(b) and the analysis given in Ref. 11], here all the closest Pb nuclei are inequivalent. This would suggest that W^{5+} (and/or Pb^{2+}) ions are significantly shifted from their symmetrical positions in the ideal PWO lattice. On the other hand, the observed shf interaction with ^{207}Pb nuclei clearly indicates that W^{5+} ions occupy regular lattice sites. Therefore the inequivalency of surrounding Pb cations can only be explained by another perturbing defect nearby.

The angular dependencies of the W^{5+} ESR lines measured in two perpendicular planes are given in Fig. 4. They are successfully described using a spin Hamiltonian of rhombic symmetry with an electron spin $S=1/2$. The fourfold site splitting observed in the spectra implies the existence of four magnetically inequivalent positions for each center. As a result, the g tensors, transforming from one into the other by the lattice symmetry operations, have different orientations. The spin Hamiltonian parameters of the centers are listed in Table I. ^{207}Pb shf tensor parameters were not determined. It was impossible due to the large number of shf lines and their relatively low intensity. For the same reason we could not reliably resolve ^{193}W hyperfine lines. However, some idea about the values of the shf splittings can be obtained from analysis presented in Fig. 3.

Based on the g-factor values (typical for a $5d^1$ electron configuration in a tetrahedral crystal-field with trigonal distortion and close to those found for the $(WO_4)^{3-}$ and $(WO_4)^{3-}$- La^{3+} centers,[11,16]) and high purity of the crystals studied (for instance, the Mo concentration was below 0.5 ppm) we ascribe the spectra in Fig. 1 to paramagnetic $W^{5+}(5d^1)$ ions which could be perturbed by some defects at the neighboring sites. The observed strong shf interaction of the electron with ^{207}Pb nuclei convincingly indicates that it is localized at the W site. In the $PbWO_4$ crystal structure a W^{6+} ion is surrounded by four closest Pb^{2+} ions (in the *ab* plane at a distance of 0.389 nm). The next nearest four Pb^{2+} ions occupy positions in the *ac* planes, or the *bc* planes at a distance of 0.409 nm. As in the case of unperturbed W^{5+} ion the largest g value, denoted g_z, is much smaller than that expected for a tetrahedral crystal field of the PWO lattice with the lowest d_{z^2} orbital. Similarly to the authors of Ref. 21, who in detail considered the $(MoO_4)^{3-}$ center, we can conclude that a large deviation from the free-electron value can be due to the large covalency contribution from the outer shells of neighboring lead cations and oxygen anions. This conclusion is further supported by the noticeable overlap of Pb and W wave functions obtained in the PWO band structure calculations[10] and namely by the anomalously strong hyperfine interaction of the paramagnetic electron with the ^{207}Pb nuclei. Another contribution to g_z comes from the excited orbitals which become nondegenerate due to the presence of perturbing defects.

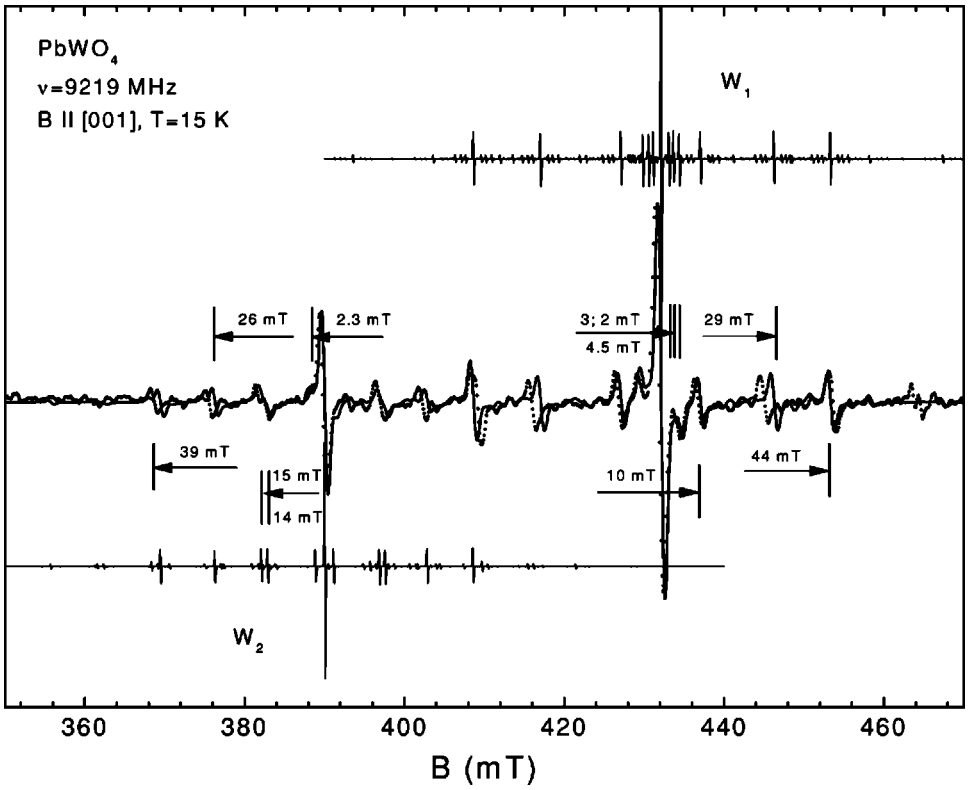

FIG. 3. Measured (points) and calculated (solid lines) ESR spectrum of the W_1 and W_2 centers for B ∥ [001] with a simulation of ^{207}Pb shf structure. The simulation was performed assuming a superhyperfine interaction of an electron with six (W_1) and five (W_2) inequivalent ^{207}Pb nuclei. Some of the calculated shf lines are slightly shifted relatively to the measured ones due to the small difference in the orientations of g and shf tensors. Upper and lower graphs represent calculated shf patterns in the limit of narrow lines to show all expected resonances.

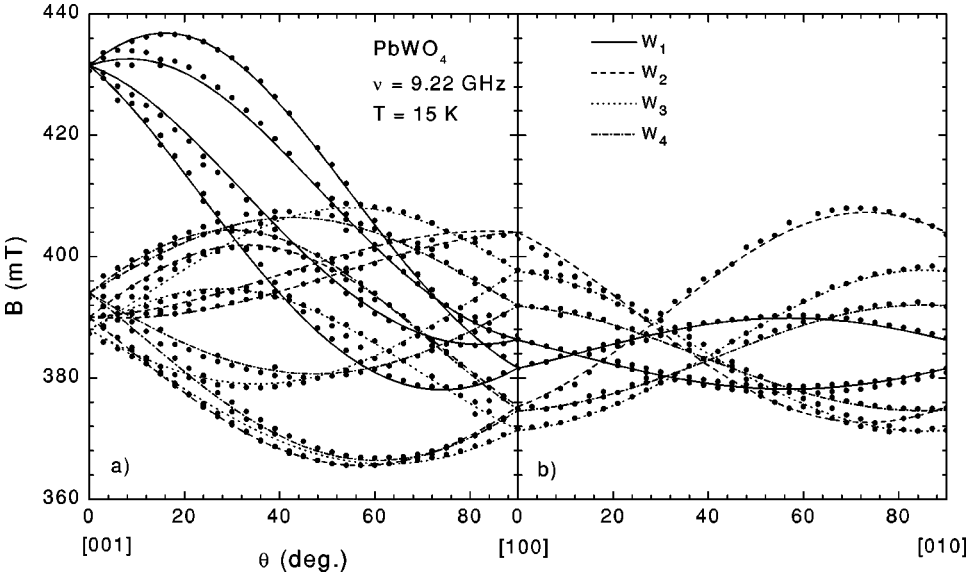

FIG. 4. Angular dependencies of W^{5+} resonances measured in (001) and (100) planes at $\nu = 9.22$ GHz and $T = 15$ K. Smooth lines correspond to calculated resonances of the W_1 center; dashed lines to the W_2 center; dotted lines to the W_3 center, and dash-dotted lines to the W_4 center. Points are experimental data.

B. Local structure of the W^{5+} centers

Because of the high purity of the $PbWO_4$ samples used, one must first consider oxygen vacancies as perturbing defects of the W sites. However, taking into account that there is more than one type of W^{5+} center, besides an oxygen vacancy one should assume the presence of another defect close to the W^{5+} ion. This additional defect is most probably located at the Pb lattice site. There are several arguments leading to the identification of $W_1, \ldots, W_4$ centers as the $(WO_3)^-$ vacancy- containing complex anions associated with a defect in the Pb sublattice $[(WO_3)^- \text{-} A_{Pb}$ complexes].

TABLE I. Spin Hamiltonian parameters for $W^{5+}(WO_3^- \text{-} A_{Pb})$ centers in $PbWO_4$. All angles are given with respect to the crystalline directions ([100],[010],[001]$\Rightarrow x,y,z$).

Center	g tensor	Polar and azimuthal angles of axes [a]		Euler angles		
		θ	φ	α	β	γ
W_1:	g_z: 1.749(1)	78	337	337	78	14
	g_y: 1.703(1)	76	70	337	−78	194
	g_x: 1.502(1)	161	28	247	78	14
				247	−78	194
W_2:	g_z: 1.809(1)	59	346	346	59	335
	g_y: 1.610(1)	111	63	346	−59	155
	g_x: 1.650(1)	141	304	256	59	335
				256	−59	155
W_3:	g_z: 1.801(1)	58	13	13	58	26
	g_y: 1.708(1)	68	117	13	−58	206
	g_x: 1.596(1)	140	55	103	58	26
				103	−58	206
W_4:	g_z: 1.803(1)	59	9	9	59	314
	g_y: 1.604(1)	128	72	9	−59	134
	g_x: 1.717(1)	127	306	99	59	314
				99	−59	134

[a]Principal axes orientation is given by polar and azimuthal angles for one of the four equivalent W^{5+} centers.

(i) In accordance with the number of oxygen ions closest to W ions (four ions), there are four magnetically inequivalent positions for each of the W^{5+} centers. Polar angles for the direction of the Z principal axes, at least for W_2, W_3, and W_4 centers, are very close to the W-O bond direction ($\theta \approx 57°$).

(ii) W^{5+} centers are not observed on PWO samples doped by trivalent ions (La^{3+}, Lu^{3+}, and Y^{3+}), which strongly suppress oxygen vacancies. On the other hand, acceptor-like impurities (Rb^+, Cu^+, and Nb^{5+}) favor the presence of these defects.

(iii) The presence of oxygen vacancies is confirmed by high-temperature treatments of the samples in oxygen atmosphere. The resulting ESR spectra are displayed in Fig. 5. One can see that the ESR signal related to W^{5+} centers practically disappeared after annealing in oxygen atmosphere. This observation supports the hypothesis that the W^{5+} centers contain an oxygen vacancy (WO_3^- centers). However, after subsequent annealing in inert Ar gas the ESR spectra did not recover their previous intensity. This could be explained by the fact that after high-temperature treatment some uncontrolled impurities, present in a low concentration, change their valence state and therefore can limit the creation of WO_3^- centers. For instance, Fig. 5 shows that the Cu^{2+} spectrum arises after annealing in oxygen atmosphere, indicating a change of copper-ion-valence state from the nonparamagnetic Cu^{1+} to paramagnetic Cu^{2+}. Furthermore, such high-temperature treatment can easily result in a space separation between oxygen vacancies and the considered defects in Pb sublattice, which leads to the destruction of $[(WO_3)^- \text{-} A_{Pb}]$ complexes.

The necessity for the presence of a second defect in the W^{5+} center model follows as well from the orientation of the g-tensor principal axes. Two of the principal axes of the W_1 center are considerably tilted from the W-O connecting line towards the ab plane ($\theta \approx 78°$; see Table I). Thus for this center we may assume either an impurity ion substituted for one of four Pb^{2+} ions arranged in square-planar symmetry or even a lead vacancy. An appearance of just three intense

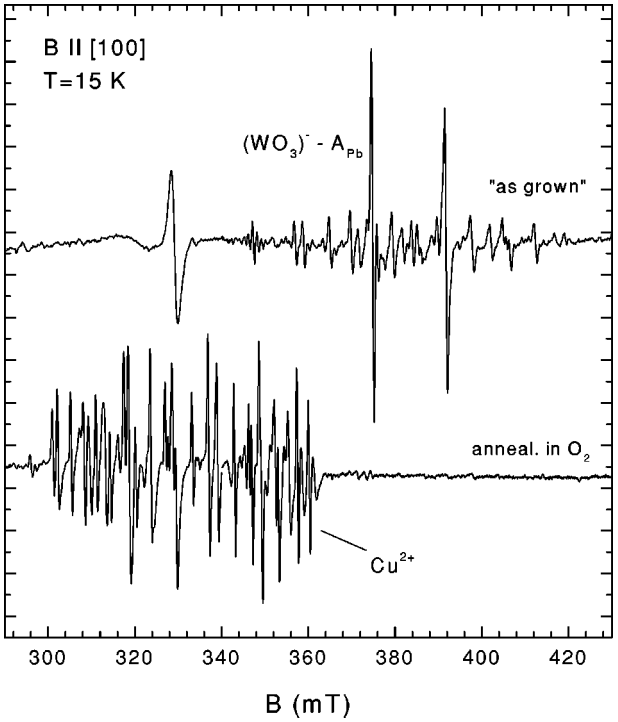

FIG. 5. Influence of a 950 °C annealing-in-oxygen treatment on the ESR signal intensity of the $(WO_3)^-$-A_{Pb} centers.

^{207}Pb shf interactions in this center also supports the model where one of the closest Pb sites is occupied by an impurity or is vacant. The main axis of the $W_2,\ldots,W_4$ centers is tilted from the W-O connecting line towards the *ac* or *bc*-planes ($\varphi \approx 10°-13°$). This means that for these centers an additional defect may be located at one of the other four more distant Pb sites arranged in D_{2d} symmetry. Based on a charge balance condition we assume that the disturbing defect should be at +1 valence state or even a lead vacancy. In fact, A^+ ions substituting Pb^{2+} (for example Rb^+ and Cu^+) favor the creation of the oxygen vacancy containing complexes because such associate pair (V_O-A^+) is energetically favorable. All possibilities of spatial arrangement of the perturbed $(WO_3)^-$ centers in the PWO lattice are schematically shown in Fig. 6.

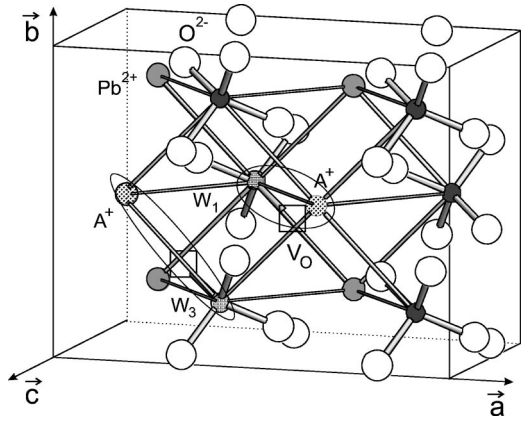

FIG. 6. Fragment of $PbWO_4$ lattice with $(WO_3)^-$-A^+ centers.

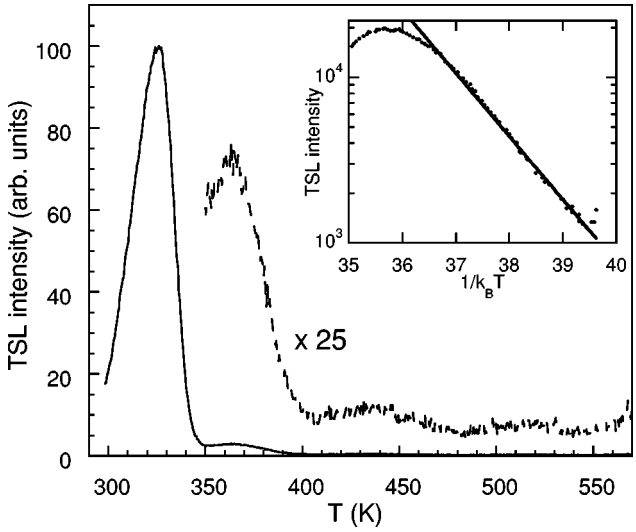

FIG. 7. TSL glow curves after x-ray irradiation at 293 K. The x-ray dose is 270 Gy (dose evaluated in air). The inset shows the Arrhenius plot of the TSL after partial cleaning at 313 K. The continuous line is an exponential fit performed on the basis of the initial rise method.

It should be noted that our analysis of the ESR spectra did not reveal (besides the ^{207}Pb shf lines) any other lines related to possible nuclear spins of the A_{Pb} pertubing ions. It could be due to too weak electron-nuclear interaction for this ion, because even lead nuclei give shf splittings which are resolved in the spectra only for 3–4 closest Pb ions. On the other hand, observed by us W^{5+} spectra cannot be ascribed to the simple $(WO_3)^-$ or $(WO_4)^{3-}$–$A_{Pb}(V_{Pb})$ defects due to difference in *g*-tensor axes orientation. For example, in calcium tungstate Z principal axis of the $(WO_3)^-$ center is pointed exactly at W-O bond direction.[22] For the $(WO_4)^{3-}$-A_{Pb} center this axis practically coincides with *c* crystal direction and other two principal axes are tilted in the *ab* plane at 45°.[16]

C. Thermal stability of $(WO_3)^-$ centers and correlation with TSL

The thermal stability of the $(WO_3)^-$ centers was investigated by measuring the time decay of their ESR intensities after ultraviolet irradiation. While at 293 K the ESR intensity of the W_3 and W_4 centers is characterized by a short decay time about 5–20 min, the W_1 and W_2 centers show a much longer decay time of about 3–5 days (Fig. 2). In order to study the role of radiative recombinations in the thermal ionization of $(WO_3)^-$ centers, TSL measurements after x-ray irradiation at 293 K were also performed. The results are displayed in Fig. 7. A dominant peak is observed at 323 K, followed by a minor peak at 365 K and by other very weak structures at higher temperatures. Wavelength-resolved TSL measurements showed that the TSL emission is centered at 2.1 eV in accordance with previous experimental results.[3] The possible correlation between the 323-K TSL peak and the oxygen-deficient centers observed here by ESR is supported by the fact that such a TSL peak is not observed in

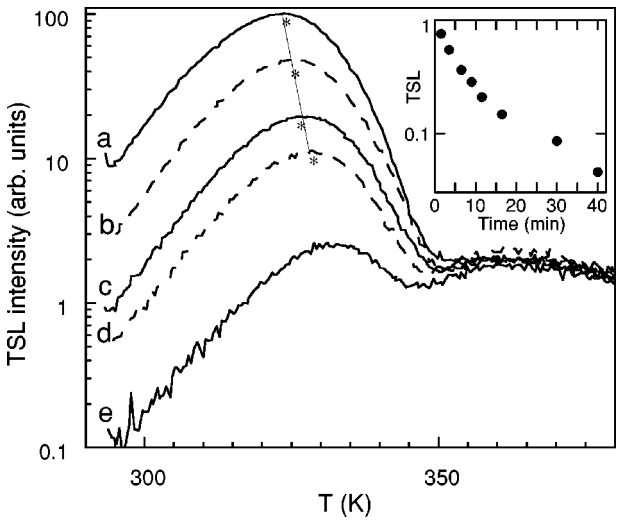

FIG. 8. TSL glow curves following different time delays after x-ray irradiation at 293 K (x-ray dose of 270 Gy, evaluated in air). (a), 1.5 min, (b), 6.5 min, (c), 16.5 min, (d), 30.5 min; and (e), 60.5 min. In the figure, the stars indicate the maximum temperatures of the peaks. The normalized intensity of the 323 K peak vs different time delays after irradiation is shown in the inset.

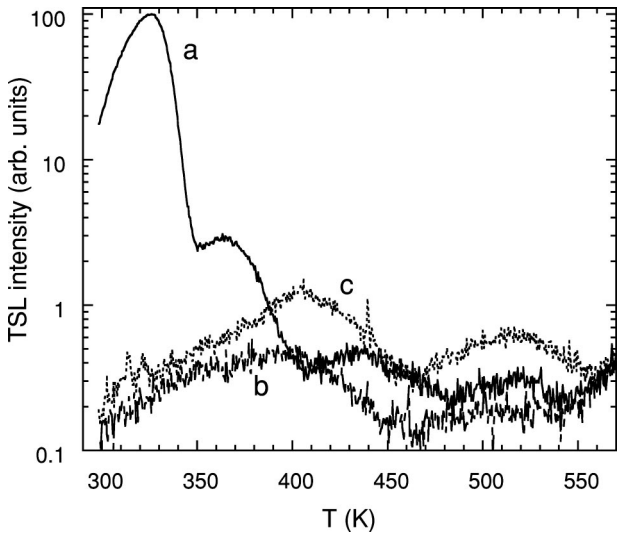

FIG. 9. TSL glow curves following x-ray irradiation at 293 K and different annealing treatments. (a), as received, (b) following annealing in an O_2 atmosphere; (c) following annealing in an O_2 atmosphere and subsequent annealing in an Ar atmosphere.

trivalent-ion-doped crystals where the concentration of oxygen vacancies should be strongly reduced.[23] The trap depth of the 323 K peak was calculated by the initial rise method applied to several glow curves obtained after irradiation and subsequent heating up to various temperatures in the 303–323-K range (partial cleaning of the glow peak). The trap depth was found to be $E=0.89\pm0.02$ eV. The inset of Fig. 7 shows an example of such evaluation. Moreover, the RT (294 K) time decay of the trap responsible for the 323-K peak was investigated by measuring the TSL glow curves following various time delays after irradiation (Fig. 8). The RT decay time of this trap is about 10 min, while the 365-K peak appears to be much more stable according to previous qualitative results where peaks in the 360–440-K region were found to have a RT decay time of the order of few days.[3] We observe that the time dependence of the intensity of the 323-K peak (see the inset of Fig. 8) is not exponential. Moreover, a slight shift of the maximum temperature of the glow peak (T_{max}) is observed by increasing the time delay after irradiation. These two experimental results might be explained by considering that either (i) the carrier recombination is governed by second order kinetics, or (ii) a composite structure of the 323-K peak exists, with at least two overlapping traps of similar depth. To get a deeper insight, we performed TSL measurements as a function of dose in the range 0.04–540 Gy. By increasing the dose in this interval, the intensity of the 323-K peak increased approximately by a factor of 50. No significant lowering of T_{max} was observed by dose increasing, contrary to what expected in the case of second order processes. As a result, the observed phenomenology is more consistent with the existence of a composite structure where at least two TSL peaks are so close in temperature that they cannot be distinguished, neither in the glow curve nor in the initial-rise evaluation. Assuming that first order recombination kinetics holds, one can calculate the frequency factor s.[24] It turned to be of the order of $10^{13}s^{-1}$. Due to the fairly good agreement between their thermal stabilities, a correlation between the W_3 and W_4 centers and the traps responsible for the composite TSL structure at 323 K can be proposed. In particular, one can propose that electrons freed from such centers undergo radiative recombination giving rise to the composite TSL peak. Although a detailed investigation of the 365-K peak was not performed because of its low intensity, a similar correlation between the trap responsible for this peak and $W_1(W_2)$ centers can also be suggested based on the similarity of their thermal stabilities. Finally, the correlation between the TSL peaks and the ESR signals of the $(WO_3)^-$ centers was supported by high-temperature-annealing treatments and green-light-illumination experiments. The 323- and 365-K TSL peaks almost disappeared (Fig. 9) after annealing in oxygen atmosphere at $T=950\,^{\circ}$C. A subsequent annealing in Ar gas did not cause the recovery of their previous intensities, similarly to what occurs in the case of ESR (Fig. 5). Moreover, the illumination of the sample with light from a tungsten halogen lamp in the 350–600-nm interval after x-ray irradiation caused a strong reduction of the 323-K peak, indicating the occurrence of photo-ionization of the TSL trap under this type of illumination.

IV. DISCUSSION

As above described, $(WO_3)^-$ -based centers are thermally stable at least up to about RT. We assume that the thermal ionization of these electron traps, rather than that of hole traps, gives rise to the TSL glow peaks at 323 and 365 K. One can easily see from Fig. 2 that under heating one $(WO_3)^-$ center transforms into another. Such a conversion is possible only when freed electrons can be retrapped by deeper traps. The statement that electrons are the mobile species in the PWO lattice is also supported by the green-light-

illumination measurements. When a crystal containing $(WO_3)^-$ centers is cooled to $T<40$ K and irradiated by the 546-nm line of an Hg arc lamp, the $(WO_3)^-$-based centers completely convert into polaronic $(WO_4)^{3-}$ centers [Fig. 1(b)]. Presumably electrons detrapped under green-light irradiation move only a short distance and become immediately localized at the polaronic $(WO_4)^{2-}$ levels rather than recombining with localized holes.

Unfortunately, the nature of hole centers in the PWO lattice is far from being established, mainly because by now no such centers have been observed by ESR. This might be connected to a very weak ESR signal due either to a strong temperature dependence of the spin-lattice relaxation of the hole centers, or more probably to the fact that these centers are not paramagnetic, e.g., a kind of bihole hypothesized in Refs. 5 and 6. In any case the hole centers should neither be simple Pb^{3+} nor O^- defects, as both of them are usually well observable by ESR, like in isostructural $CaWO_4$.[25,26] At the same time the results presented here definitely rule out the hypothesis about the nature of electron traps participating in radiation damage processes given in Ref. 3 (simple F and F^+ centers) and probably also in Ref. 5 (oxygen bivacancy centers), because all the W^{5+} centers configurations point to the combination of an oxygen vacancy and a defect in the Pb cation surroundings.

Following the above presented data on the $(WO_3)^-$-based centers together with analogous data of $(WO_4)^{3-}$ and Pb^+-V_O centers (see Refs. 11 and 15) we can propose a global scheme of local electronic levels in the band gap of PWO, which are associated with all these electron traps. The scheme is depicted in Fig. 10. Ultraviolet (330 nm) or x-ray irradiation at $T\lesssim 40$ K usually creates intrinsic $(WO_4)^{3-}$ electronic centers and some hole centers of an unknown origin. The energy level of the $(WO_4)^{3-}$ center is located 50 meV below the bottom of the conduction band (CB). At about 50 K the electrons are thermally freed from the $(WO_4)^{3-}$ centers and radiatively recombine with holes localized nearby, giving rise to the excitonlike emission in the blue spectral region detected by TSL. However, a significant portion of freed electrons can be retrapped by deeper electron traps: $(WO_4)^{3-}$-La^{3+}(Y^{3+}), Pb^+-V_O, $(MoO_4)^{3-}$, $(WO_3)^-$-A^+, etc. depending on the purity and/or doping of the crystal. As evidenced both from ESR and TSL measurements, the energy level of $(WO_4)^{3-}$-La^{3+} centers is located 0.27 eV below the bottom of the CB.[16] The corresponding energies of Pb^+-V_O and (more shallow) $(WO_3)^-$-A^+ centers are 0.55 eV and about 0.9 eV, respectively. At the temperature where such electron traps are thermally ionized the TSL glow peaks arise and indicate the radiative recombination of part of the freed electrons at hole centers. The remaining electrons are retrapped by deeper traps increasing their concentration as it is seen from Fig. 10. The most stable part of the $(WO_3)^-$-A^+ centers evidenced in this study survive at room temperature typically for several days and could be also considered responsible for part of the radiation induced optical absorption well-known from radiation damage studies.

It is worth noting that we did not find unperturbed $(WO_3)^-$ centers in any of the crystals studied. This may be

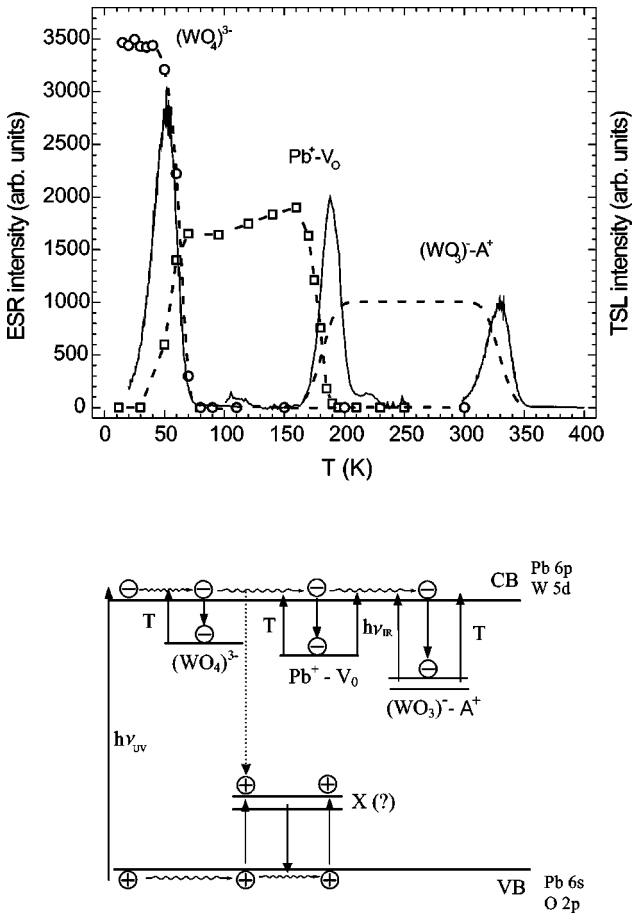

FIG. 10. Comparison between TSL peaks and the thermal stability of photoinduced centers monitored by ESR. Points and dashed lines are ESR intensities, and solid lines depict TSL intensities. The bottom panel represents the energy level diagram.

related to the fact that in the PWO structure both W^{6+} and Pb^{2+} ions are able to attract an electron trapped around a neighboring oxygen vacancy. It is known that in PWO the bottom of conduction band is formed by both 5d states of the W^{6+} ion and $6p$ states of the Pb^{2+} ion (see Refs. 10 and 27). It seems thus difficult to predict which configuration of $(WO_3)^-$ or Pb^+-V_O would be energetically more preferable. Theoretical calculations[9] predict the level of $(WO_3)^-$ to lie more than 0.7 eV below the conduction-band edge, while the Pb^+-V_O defect energy configuration was not found at all. On the other hand, from the present experiment we find that for the $(WO_3)^-$-A^+ center the electron binding energy is about 0.9 eV. For the simple $(WO_3)^-$ center this binding energy has to be smaller. Hence it may become comparable to that of Pb^+-V_O configuration ($\sim$0.55 eV, Ref. 15), supporting the idea of the competition between these two traps of similar depth (with possible dominance of Pb^+-V_O) in the electron capture. Furthermore, in Ref. 9 it was concluded that a Pb–O vacancy pair introduces even two density-of-state peaks in the PWO band gap associated with W^{6+}. It seems probable that after electron capture such center may be even a deeper electron trap with respect to a simple $(WO_3)^-$. Therefore, in some aspects these theoretical calculations of the energy structure of oxygen-vacancy-based defects in

PWO qualitatively agree with experimental results presented in this work.

V. CONCLUSIONS

Four different types of deep electron traps were identified by ESR measurements performed on $PbWO_4$ single crystals of high purity irradiated by ultraviolet light or x-rays at room temperature. Electrons are trapped at tungsten ions associated with complex defects like oxygen vacancies coupled to other defects located at surrounding Pb sites. The occurrence of two pairs of such traps with significantly different stability at room temperature (about 10 min. and four days) correlates with the occurrence of two groups of Pb-site defects located at slightly different distances, 0.3888 and 0.4092 nm, from the central tungsten ion. Monovalent-impurity ions and lead vacancies represent possible candidates for the Pb-site defects. Electrons thermally freed from these traps are responsible for thermoluminescence peaks at 323 K and around 365 K. The similar temperature stabilities and the similar dependences of the signals from high-temperature annealing and light illumination further support the correspondence between the centers observed in ESR and TSL glow peaks.

ACKNOWLEDGMENTS

This research was supported by the NATO Science for Peace Project No. 973510-Scintillators, Czech GA CR 202/01/0753 and ME447 projects.

[1] CMS technical proposal CERN/LHCC 94-38, LHCC/P1 (1994) and ALICE Technical Proposal CERN/LHCC 95-71, LHCC/P3 (1995).
[2] M. Nikl, Phys. Status Solidi A **178**, 595 (2000).
[3] M. Nikl *et al.*, J. Appl. Phys. **82**, 5758 (1997).
[4] R. Y. Zhu *et al.*, IEEE Trans. Nucl. Sci. **NS-45**, 686 (1998).
[5] A. Annenkov, E. Auffray, M. Korzhik, P. Lecoq, and J.-P. Peigneux, Phys. Status Solidi A **170**, 47 (1998).
[6] Q. Lin, X. Feng, and Z. Man, Solid State Commun. **118**, 221 (2001).
[7] Q. Lin, X. Feng, and Z. Man, Phys. Status Solidi A **181**, R1 (2000).
[8] Q. Lin, X. Feng, and Z. Man, Phys. Rev. B **63**, 134 105 (2001).
[9] Y. B. Abraham, N. A. W. Holzwarth, R. T. Williams, and G. E. Matthews, Phys. Rev. B **64**, 245 109 (2001).
[10] N. A. W. Holzwarth, Y. Zhang and R. T. Williams, in *Tungstate Crystals*, edited by S. Baccaro, B. Borgia, I. Dafinei, and E. Longo (Universitá degli Studi La Sapienza, Rome, 1999), p. 103. ISBN 88-87242-10-0.Proc. of the Int.workshop on Tungstate Crystals, Rome, Italy, Oct 12-14, 1998.
[11] V. V. Laguta, J. Rosa, M. I. Zaritskii, M. Nikl, and Y. Usuki, J. Phys.: Condens. Matter **10**, 7293 (1998).
[12] M. Bohm, F. Henecker, A. Hofstaetter, M. Luh, B. K. Meyer, A. Scharmann, O. V. Kondratiev, and M. V. Korzhik, Radiat. Eff. Defects Solids **150**, 21 (1999).
[13] M. Martini, F. Meinardi, G. Spinolo, A. Vedda, M. Nikl, and Y. Usuki, Phys. Rev. B **60**, 4653 (1999).
[14] A. Hofstaetter, M. V. Korzhik, V. V. Laguta, B. K. Meyer, V. Nagirnyi, R. Novotny, Radiat. Meas. **33**, 533 (2001).
[15] V. V. Laguta, M. Martini, A. Vedda, M. Nikl, E. Mihóková, P. Bohaček, J. Rosa, A. Hofstaetter, B. K. Meyer, and Y. Usuki, Phys. Rev. B **64**, 165 102 (2001).
[16] V. V. Laguta, M. Martini, F. Meinardi, A. Vedda, M. Nikl, E. Mihóková, J. Rosa, A. Hofstaetter, B. K. Meyer, and Y. Usuki, Phys. Rev. B **62**, 10 109 (2000).
[17] A. Hofstaetter, H. Alves, M. Bohm, D. M. Hofmann, O. V. Kondratiev, M. V. Korzhik, V. V. Laguta, M. Luh, V. Metag, B. K. Meyer, R. Novotny, N. G. Romanov, A. Scharmann, A. Vedda, and A. Watterich, in *Proceedings of the Fifth International Conference on Inorganic Scintillators and Their Applications, Moscow, August 16-20, 1999*, edited by V. Mikhailin (Lomonosov State University, Moscow, 2000), pp. 128–136.
[18] V. V. Laguta, M. Martini, A. Vedda, E. Rosetta, M. Nikl, E. Mihóková, P. Bohaček, J. Rosa, A. Hofstaetter, B. K. Meyer, and U. Usuki, Radiat. Eff. Defects Solids **157**, 1025 (2002).
[19] M. Kobayashi *et al.*, Nucl. Instrum. Methods Phys. Res. A **373**, 333 (1996).
[20] J. Rosa, H. R. Asatryan, and M. Nikl, Phys. Status Solidi A **158**, 573 (1996).
[21] A. Hofstaetter, A. Scharmann, D. Schwabe, and B. Vitt, Z. Phys. B **30**, 3055 (1978).
[22] K. C. Chu and C. Kikuchi, Phys. Rev. **169**, 752 (1968).
[23] S. Baccaro, P. Bohacek, B. Borgia, A. Cecilia, I. Dafinei, M. Diemoz, M. Ishii, O. Jarolimek, M. Kobayashi, M. Martini, M. Montecchi, M. Nikl, Y. Usuki, and A. Vedda, Phys. Status Solidi A **160**, R5 (1997).
[24] S. W. S. Mc Keever, *Thermoluminescence of Solids* (Cambridge University Press, Cambridge, 1985).
[25] R. Biederbick, G. Born, A. Hofstaetter, and A. Scharmann, Phys. Status Solidi B **69**, 55 (1975).
[26] G. Born, A. Hofstaetter, and A. Scharmann, Phys. Status Solidi **37**, 255 (1970).
[27] Y. Zhang, N. A. W. Holzwarth, and R. T. Williams, Phys. Rev. B **57**, 12 738 (1998).